# Supporting Information

## Polycrystalline soft carbon semi-hollow microrod anode for advanced K-ion full batteries

Xuanpeng Wang, [a] Kang Han, [a] Dongdong Qin, [a] Qi Li,*[a] Chenyang Wang,[a] Chaojiang Niu,[a] Liqiang Mai *[ab]

a. State Key Laboratory of Advanced Technology for Materials Synthesis and Processing, Wuhan University of Technology, Wuhan 430070, China

b. Department of Chemistry, University of California, Berkeley, California 94720, United States

Email: mlq518@whut.edu.cn; qi.li@whut.edu.cn

**Key words:** Semi-hollow microrod, K-ion full batteries, soft carbon, high-capacity, polycrystalline, *in-situ* X-ray diffraction

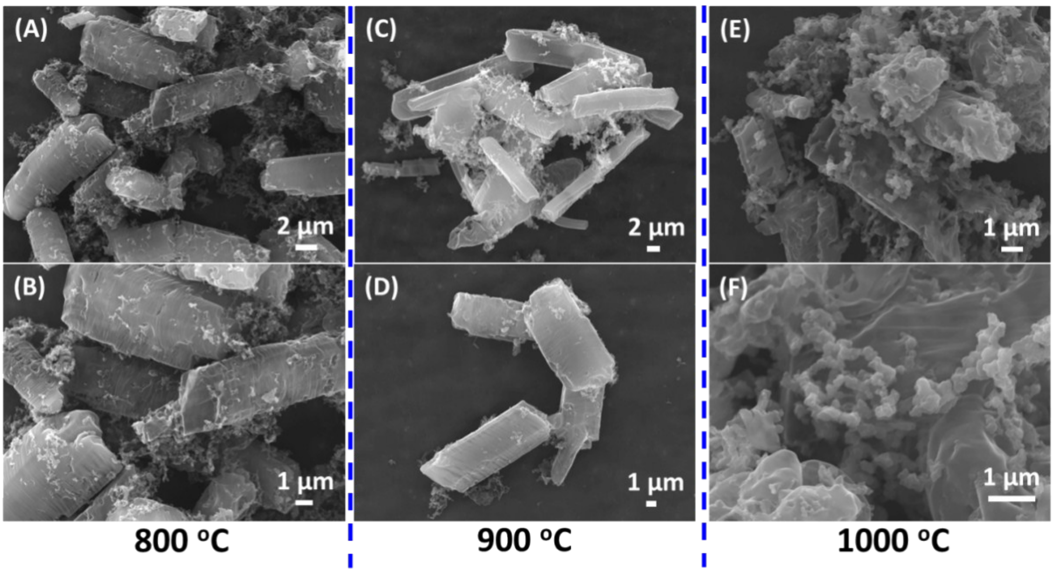


**Figure S1.** SEM images of the soft carbon sintered at 800 °C (A, B), 900 °C (C, D), 1000 °C (E, F).

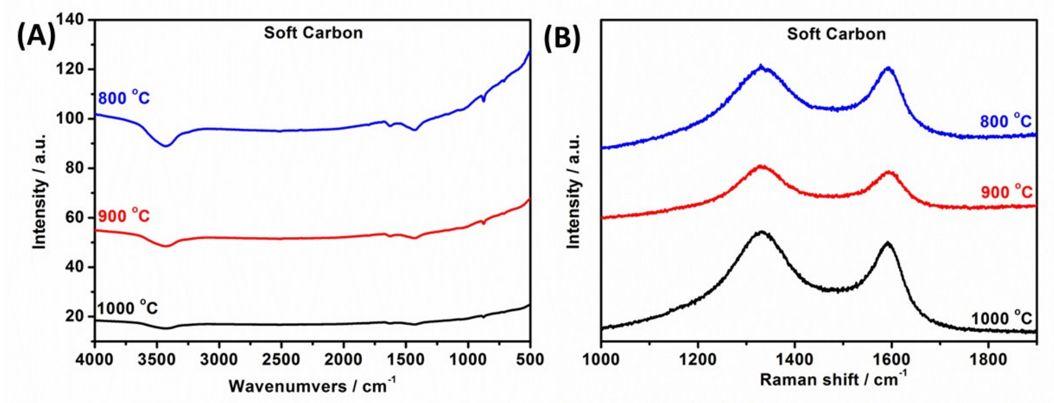


**Figure S2.** FT-IR spectra (A) and Raman spectra (B) of the three soft carbon samples.

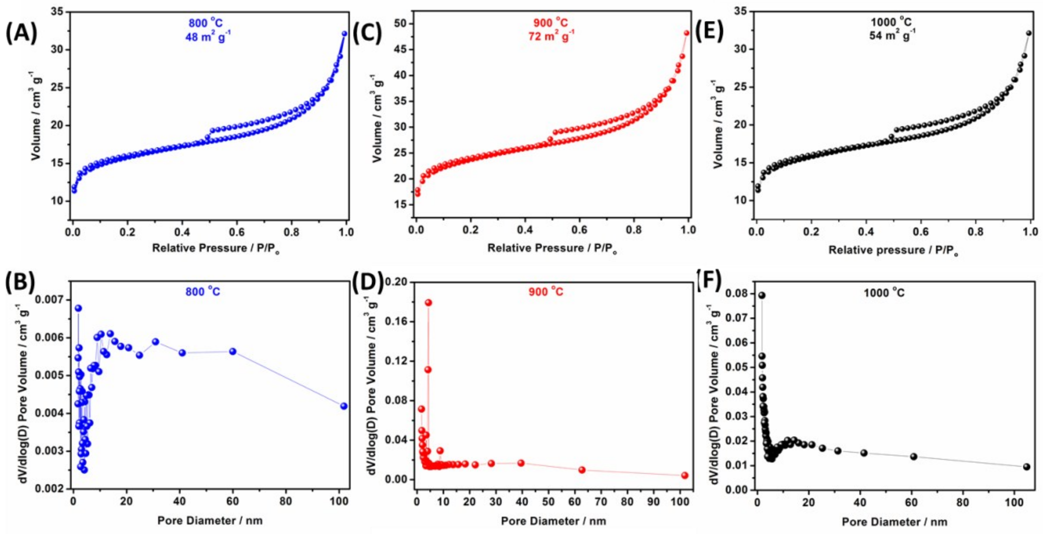


**Figure S3.** The nitrogen adsorption-desorption isothermsand pore size distribution (B) of the soft carbon sintered at 800 °C (A, B), 900 °C (C, D) and 1000 °C (E, F), respectively.

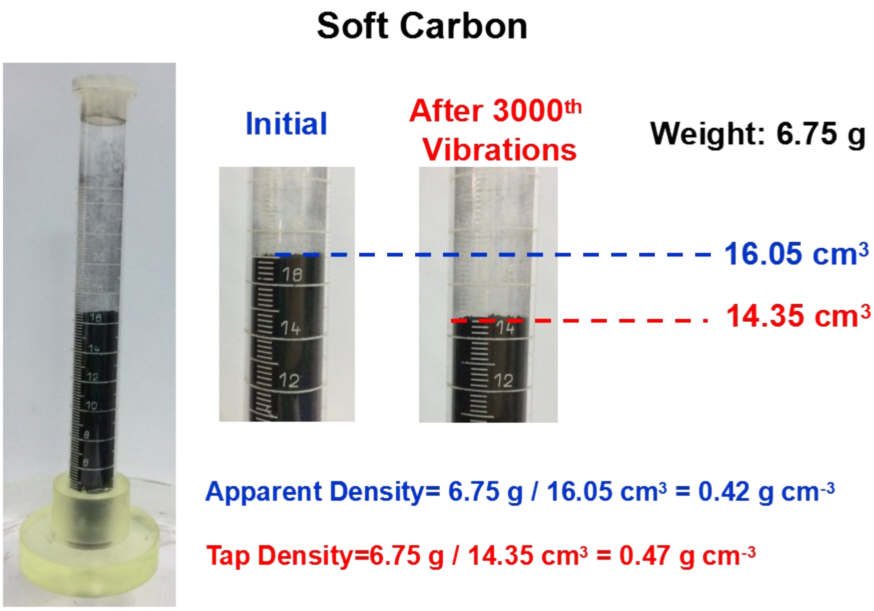


**Figure S4**. The tap density and apparent density test of soft carbon sintered at 900 °C .

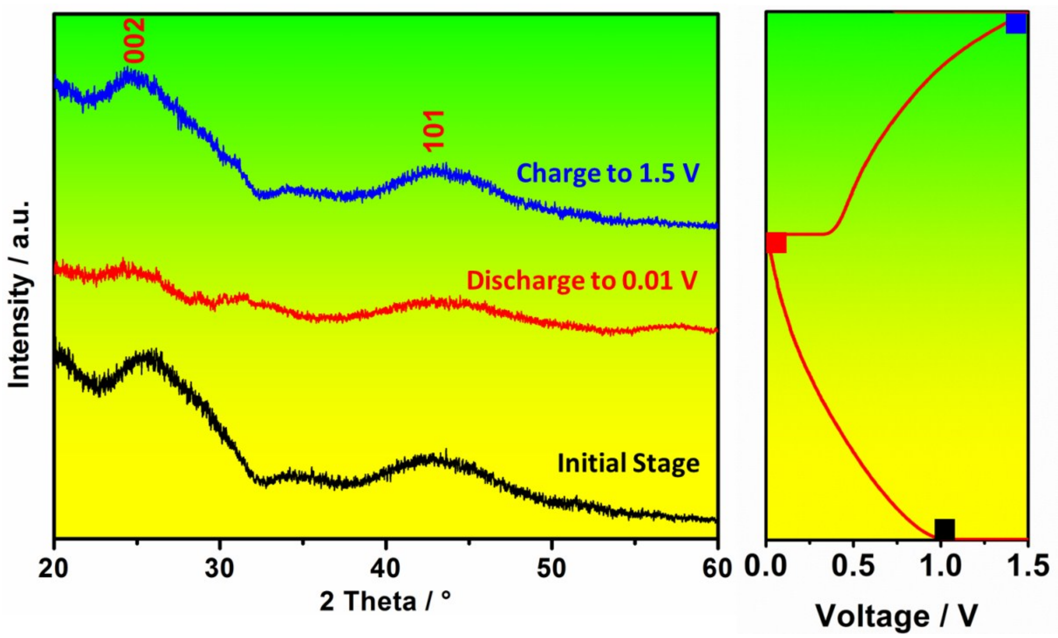


**Figure S5.** *Ex*-situ XRD patterns at different stages of the soft carbon sintered at 900 °C.

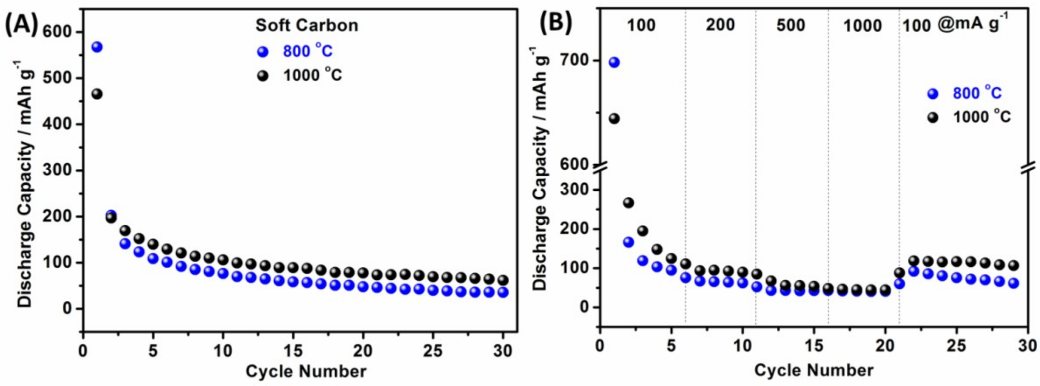


**Figure S6.** Cycling performance (A) and rate performance (B) of the soft carbon samples sintered at 800 °C and 1000 °C, respectively.

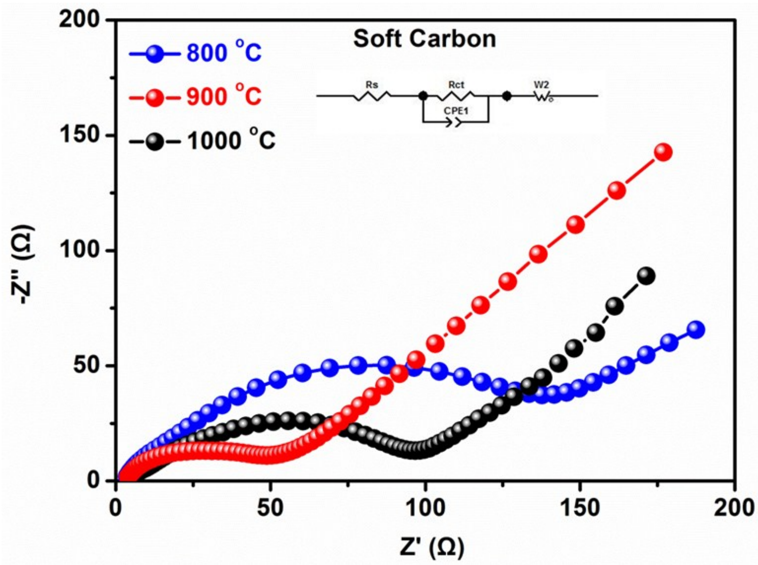


**Figure S7.** AC impedance plots of the three soft carbon samples before cycling (from 0.1Hz to 100 kHz).

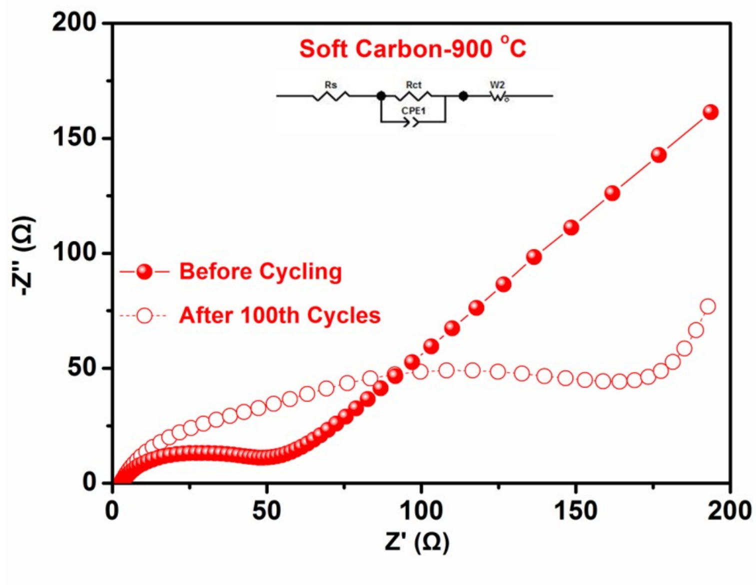


**Figure S8.** AC impedance plots of the three soft carbon sintered at 900 °C before cycling and after the 100th cycle at the current density of 100 mA $g^{-1}$ (from 0.1Hz to 100 kHz).

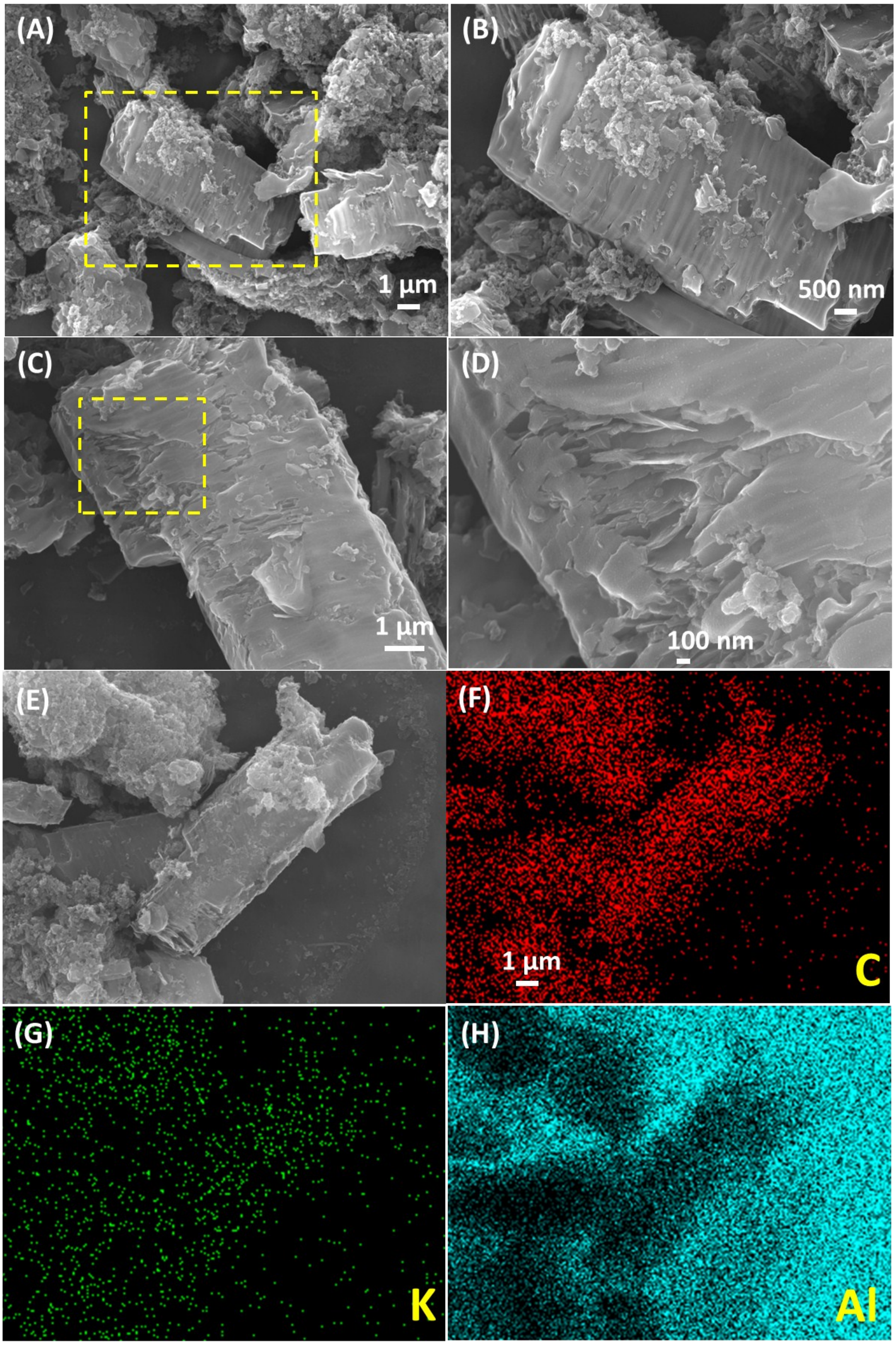


**Figure S9.** SEM images (A-D) and EDS mappings (E-H) of the soft carbon sintered at 900 °C, after 100 cycles at 100 mA $g^{-1}$ in K-ion batteries.

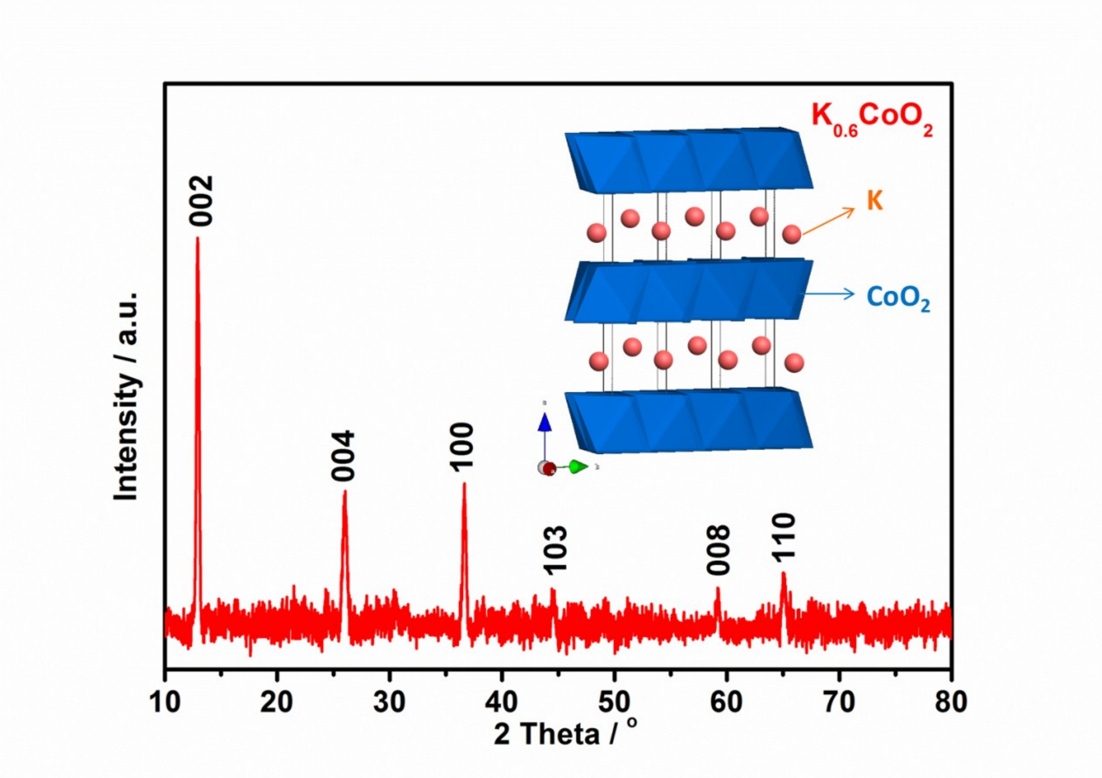


**Figure S10.** XRD pattern and schematic diagram of the crystal structure of $K_{0.6}CoO_2$ interconnected nanoparticles.

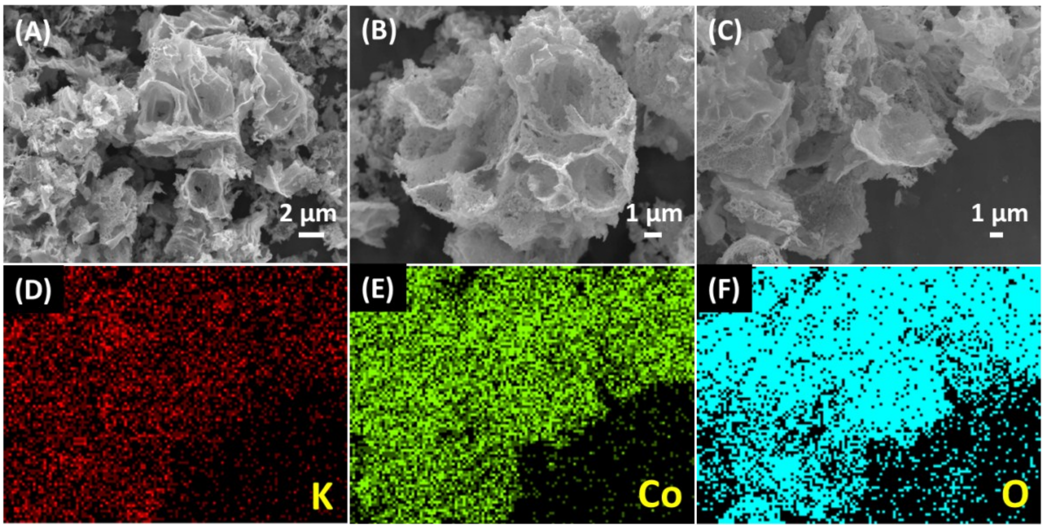


**Figure S11.** SEM images (A-C) and EDS mappings (D-F) of the $K_{0.6}CoO_2$ interconnected nanoparticles.

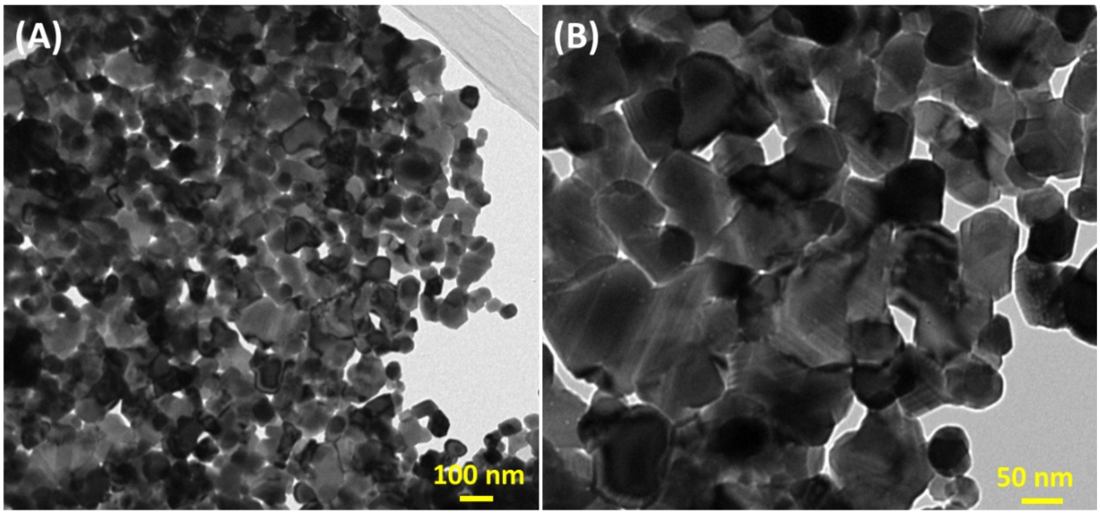


**Figure S12.** TEM images of the $K_{0.6}CoO_2$ interconnected nanoparticles.

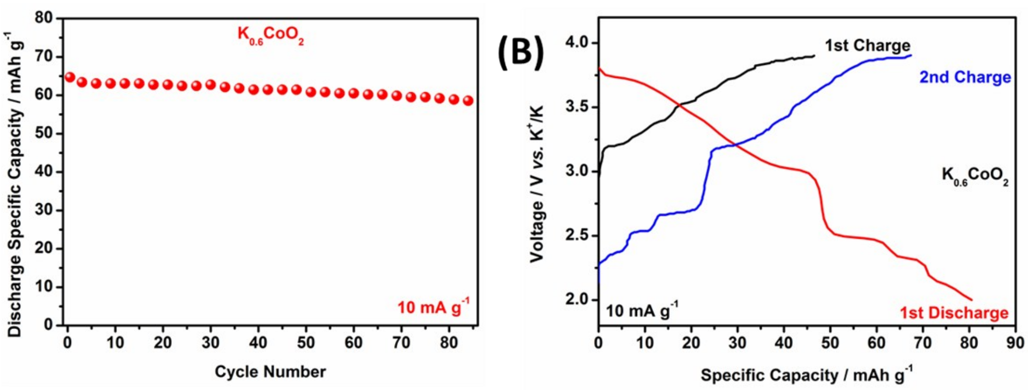


**Figure S13.** Cycling performance (A) and depotassiation/potassiation curves (B) of the $K_{0.6}CoO_2$ interconnected nanoparticles when test as a cathode in KIBs, respectively.

**Table S1.** Comparison of the electrochemical performances of carbon-based anode materials in non-aqueous KIBs.

| Active materials | Voltage ranges (V) | Current density (mA $g^{-1}$) | 2th cycle capacity (mAh $g^{-1}$) | Cycle numbers | Capacity retention |
|---|---|---|---|---|---|
| **Semi-hollow microrod soft carbon (This work)** | 0.01-1.5 | 100 | 312 | 100 | 80% |
| | | 500 | 214 | 500 | 82% |
| **Graphite[23]** | 0.01 - 1.5 | 150 | 245 | 50 | 45% |
| **Soft carbon[23]** | 0.01 - 1.5 | 500 | 210 | 20 | 74% |
| **Polynanocrystalline graphite[25]** | 0.1-2.0 | 100 | 170 | 300 | 50% |
| **Hard–soft composite carbon[26]** | 0.01-2.0 | 270 | 200 | 200 | 93% |